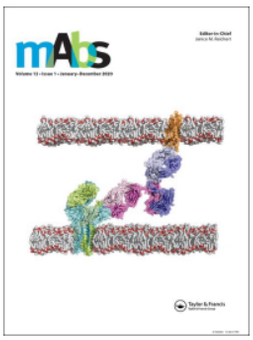

mAbs

ISSN: (Print) (Online) Journal homepage: https://www.tandfonline.com/loi/kmab20

Dose escalation PET imaging for safety and effective therapy dose optimization of a bispecific antibody

Yan Wang, Donghui Pan, Chenrong Huang, Bingliang Chen, Mingzhu Li, Shuaixiang Zhou, Lizhen Wang, Min Wu, Xinyu Wang, Yicong Bian, Junjie Yan, Junjian Liu, Min Yang & Liyan Miao

To cite this article: Yan Wang, Donghui Pan, Chenrong Huang, Bingliang Chen, Mingzhu Li, Shuaixiang Zhou, Lizhen Wang, Min Wu, Xinyu Wang, Yicong Bian, Junjie Yan, Junjian Liu, Min Yang & Liyan Miao (2020) Dose escalation PET imaging for safety and effective therapy dose optimization of a bispecific antibody, mAbs, 12:1, 1748322, DOI: 10.1080/19420862.2020.1748322

To link to this article: https://doi.org/10.1080/19420862.2020.1748322

MABS
2020, VOL. 12, NO. 1, e1748322 (10 pages)
https://doi.org/10.1080/19420862.2020.1748322

Taylor & Francis
Taylor & Francis Group

REPORT

Dose escalation PET imaging for safety and effective therapy dose optimization of a bispecific antibody

Yan Wang[a,b]*, Donghui Pan[c]*, Chenrong Huang[a,b]*, Bingliang Chen[d], Mingzhu Li[c], Shuaixiang Zhou[d], Lizhen Wang[c], Min Wu[d], Xinyu Wang[c], Yicong Bian[a,b], Junjie Yan[c], Junjian Liu[d], Min Yang[c], and Liyan Miao[a,b]

[a]Department of Clinical Pharmacology, The First Affiliated Hospital of Soochow University, Suzhou, China; [b]Institute for Interdisciplinary Drug Research and Translational Sciences, College of Pharmaceutical Sciences, Soochow University, Suzhou, China; [c]NHC Key Laboratory of Nuclear Medicine, Jiangsu Key Laboratory of Molecular Nuclear Medicine, Jiangsu Institute of Nuclear Medicine, Wuxi, Jiangsu, China; [d]Drug Discovery Department, Innovent Biopharmaceutical (Suzhou) Co., Ltd, Suzhou, China

ABSTRACT

Selecting the dose for efficacy and first-in-human studies of bispecific antibodies (BsAbs) is a challenging process. Herein, positron emission tomography (PET) imaging with ^{89}Zr-labeled IBI322, an anti-CD47/PD-L1 BsAb, was used to optimize the safety and effective therapy dose. By labeling with ^{89}Zr, we aimed to assess the pharmacokinetics (PK), safety, and target engagement of IBI322 with dose escalation dynamic PET imaging in humanized transgenic animal models bearing MC38 tumors (knock-in of hCD47 and hPDL1). ^{89}Zr-labeled IBI322 specifically accumulated in tumors with a tumor-to-muscle ratio of 12.37 ± 1.42 at 168 h (0.22 mg/kg) and the biodistribution of normal tissues from PET imaging could be used for preliminary safety prediction. According to the Pearson correlation analysis between the ELISA-quantified serum concentration and heart uptake (%ID/g) (r = 0.980), a modified Patlak model was proposed. The exploratory target-mediated 50% (0.38 mg/kg) and 90% (0.63 mg/kg) inhibitory mass doses were calculated with the current modified Patlak model. The preliminary pharmacodynamics (PD) study with 0.34 mg/kg revealed that the dose prediction was rational. In conclusion, dose escalation PET imaging with ^{89}Zr-labeled antibodies is promising for PK/PD modeling and safety prediction, and helpful for determining rational dosing for preclinical and clinical trials of BsAbs.

ARTICLE HISTORY
Received 6 January 2020
Revised 26 February 2020
Accepted 24 March 2020

KEYWORDS
^{89}zr-immunoPET; bispecific antibodies; target engagement; dose selection

Introduction

For tumor immunotherapy using any antibody drugs, it is critical to define the optimal dose for future efficacy and first-in-human (FIH) studies. Their anti-tumor effects rely on the specific recognition of the target receptor, and receptor saturation generally occurs during dose escalation. Administration of an amount above the saturation dose is not expected to provide additional therapeutic benefit, but may increase the risk of adverse reaction and toxicity. Therefore, using the maximum tolerated dose method applied to small-molecule cytotoxic agents is not suitable for antibody drugs.[1]

Currently, the biologically effective dose (BED) concept is used for the selection of antibody dosing in clinical settings. Target engagement assessment is an important parameter for optimizing the BED of antibodies and antibody conjugates, and it can be used to construct pharmacokinetic/pharmacodynamic (PK/PD) models bridging animal and human testing.[1–5] Flow cytometry,[5–8] enzyme-linked immunosorbent assays (ELISAs),[9] and mass spectrometry[10] are commonly employed to measure the target saturation of monoclonal antibody (mAb) binding to the receptors of circulating blood cells, and immunohistochemistry (IHC) is usually used to assess the selective localization of target proteins in tissue specimens.[8,11]

Studies have shown that molecular imaging can be used to assess target engagement.[12–14] In 2017, Alsaid et al. investigated GSK2849330 HER3 receptor occupancy in HER3-positive xenograft tumors (BxPC3, and CHL-1) by near-infrared fluorescence optical imaging.[12] Another report by Burvenich et al. showed that gamma camera imaging of the ^{111}In-labeled anti-DR 5 antibody CS-1008 can be used to measure DR5 target saturation in vivo.[13] In addition, due to its high sensitivity, high resolution, excellent quantitative performance and ability to bridge preclinical and clinical research, positron emission tomography (PET) imaging has become a powerful imaging modality for antibody drug development. In this context, the technique is also known as immunoPET.[15] ^{89}Zirconium (^{89}Zr, $T_{1/2}$: 78.4 h, Emean: 385 KeV) is an ideal radionuclide for immunoPET (^{89}Zr-ImmunoPET). Similar to single-photon emission computed tomography,[16] ^{89}Zr-ImmunoPET has several advantages compared to the traditional method. First, the noninvasive approach can avoid blood collection for flow cytometry analysis, which might be difficult to consecutively obtain in small animal models.[8,15] Second, it can provide real-time and accurate systemic antibody IHC imaging of the whole body simultaneously,

CONTACT Min Yang yangmin@jsinm.org NHC Key Laboratory of Nuclear Medicine, Jiangsu Key Laboratory of Molecular Nuclear Medicine, Jiangsu Institute of Nuclear Medicine, 20 Qianrong Road, Wuxi Binhu District, Wux,Jiangsu 214063, China; Liyan Miao miaolysuzhou@163.com Department of Clinical Pharmacology, The First Affiliated Hospital of Soochow University, 899 Pinghai Road, Suzhou Gusu District, Suzhou, Jiangsu 215006, China
*These authors contributed equally.

Supplemental data for this article can be accessed on the publisher's website.

not only for all tumor lesions and their metastases but also for normal tissues, such as the spleen, which is an immune organ that is expected to predict the safety of antibody immunotherapy.[17]

In addition to its use in PK investigations of mAbs,[18] including BsAbs[19,20] and antibody-drug conjugates (ADCs),[21] recent studies[1,4,13] have shown that the target engagement for mAbs can be assessed by PET. The assessment of BsAbs, however, is more urgent and difficult than that for canonical (i.e., monospecific) mAbs. First, analytical methods may need to be combined or modified in order to quantify more than one target, which would be more complicated than the methods used for monospecific mAbs. Second, because of the greater cytotoxicity of bispecifics such as the T-cell engaging molecules compared to canonical mAbs,[22] target saturation, and safety assessment are more urgent for the transition to clinical studies.

Dose selection for FIH studies of IBI322, the first anti-CD47 /PD-L1 checkpoint BsAb approved by the National Medical Products Administration for clinical trials (IND No. CXSL1900125), was assessed in this study. However, similar to most other BsAbs and ADCs, the lower dosages and narrower therapeutic windows compared to canonical mAbs created many challenges. Reasonable evaluation of the safety and effectiveness of this type of antibody is an important issue. Herein, a noninvasive approach consisting of PET imaging with ^{89}Zr-labeled IBI322 was used to investigate the PK, target saturation and safety assessment for rational dose selection with a modified Patlak model. Additionally, a preliminary PD study was performed to investigate the rationality of the exploratory results for therapeutic dose selection.

Results

Conjugation and radiolabelling

The size exclusion chromatography (SEC)-high-performance liquid chromatography (HPLC) results indicate that the chemical purity of Df-IBI322 was >98% (Supplemental Figure 2a). The affinity results show that Df-IBI322 has a high affinity for human PD-L1 and human CD47, with equilibrium dissociation constants (K_D) of $1.35*10^{-8}$ M and $1.29*10^{-9}$ M, respectively (Supplemental Figure 2c).

Df-IBI322 was successfully radiolabelled with ^{89}Zr with excellent yields (>85%; non-decay corrected) and high radiochemical purity (>99%) (Supplemental Figure 2b). High specific activities (SA) of ^{89}Zr-labeled IBI322 (~45 GBq/μmol) were achieved. The stability values of ^{89}Zr-labeled IBI322 in acetate buffer at 4°C for 168 h and in human serum at 37°C for 72 h were greater than 90% (Supplementary Figure 3a, b).

Dose escalation PET imaging study

Minimal uptake was found in muscle and brain tissues for every dosage within 168 h, and the uptake (%ID/g) of the brain and muscle was generally the same: ~0.7–1.0 after 96 h. Radioactivity accumulated in the tumor, liver, and spleen (Figure 1(a) and Supplementary Figure 4).

Tumor uptake reached a steady state at 48 h for all groups, and specific accumulation was found in the tumor for doses less than 2 mg/kg, with values of 9.36 ± 1.41 for group 1 (0.22 mg/kg) and 7.41 ± 1.56 for group 2 (0.5 mg/kg) at 168 h. No statistically significant differences appeared among the doses greater than 2 mg/kg, with values of 4.95 ± 1.49 for group 3 (2 mg/kg) and 4.52 ± 0.78 for group 5 (32 mg/kg) at 168 h (Figure 1(c)). Furthermore, the normalized tumor-to-muscle ratios were significantly higher at the doses of 0.22 mg/kg (12.37 ± 1.42) and 0.5 mg/kg (9.45 ± 0.46) than in the other three groups (6.48–7.27) (Figure 1(d)).

As CD47 expression is ubiquitous in red blood cells (RBCs), the heart is an important region of interest (ROI) to evaluate the PK and biodistribution of IBI322. The highest amount of heart uptake (%ID/g) occurred for all groups at 2 h, but the uptake decreased with dose escalation, from 25.04 ± 0.80 (0.22 mg/kg) to 14.29 ± 1.95 (32 mg/kg), after which the heart uptake (%ID/g) gradually decreased with time for each group (Figure 1(b)). The area under the equivalent concentration-time curve (AUC) was linearly related to the dosage, while the half-life (t1/2) increased slightly as the dose escalated (Supplemental Figure 4), which was similar to the results of other mAbs.[17]

Consistent with the heart uptake, as a type of tissue with abundant blood content, the overall trend of initial accumulation in the liver gradually decreased from group 1 (0.22 mg/kg) to group 5 (32 mg/kg), and the liver radioactive clearance rate gradually decreased from 26.83 ± 4.16 (2 h, n = 4) to 13.39 ± 0.61 (168 h, n = 4), $p = .001$, for group 1 (0.22 mg/kg), and from 18.28 ± 0.82 (2 h, n = 3) to 14.80 ± 1.35 (168 h, n = 3), $p < .05$, for group 5 (32 mg/kg) (Figure 1(e)).

Interestingly, as another tissue with abundant blood content, the trends of spleen uptake were not the same among the groups. In groups 1 through 3, in which the injection dose was less than 2 mg/kg, spleen uptake gradually decreased after administration. At a dose of 8 mg/kg, radioactive uptake in the spleen remained stable from 2 h to 168 h. However, for the highest dose of 32 mg/kg in group 5, spleen uptake gradually increased from 8.32 ± 0.55 (2 h, n = 3) to 11.70 ± 0.20 (168 h, n = 3), $p < .01$ (Figure 1(f)).

Safety

No abnormalities in body weight were observed among the different groups (Figure 2(a)). However, one animal in the highest dose group (32 mg/kg) died during the 168 h of monitoring.

Hematoxylin/eosin (H&E) staining showed no abnormal hepatocyte morphology at each dose, while slight changes in the morphology of the spleen, with partial necrosis in the animal that died, occurred at the highest dosage (Figure 2(b)).

Biodistribution

The biodistribution results were consistent with the PET imaging results in the 0.5 mg/kg group, and tumor uptake

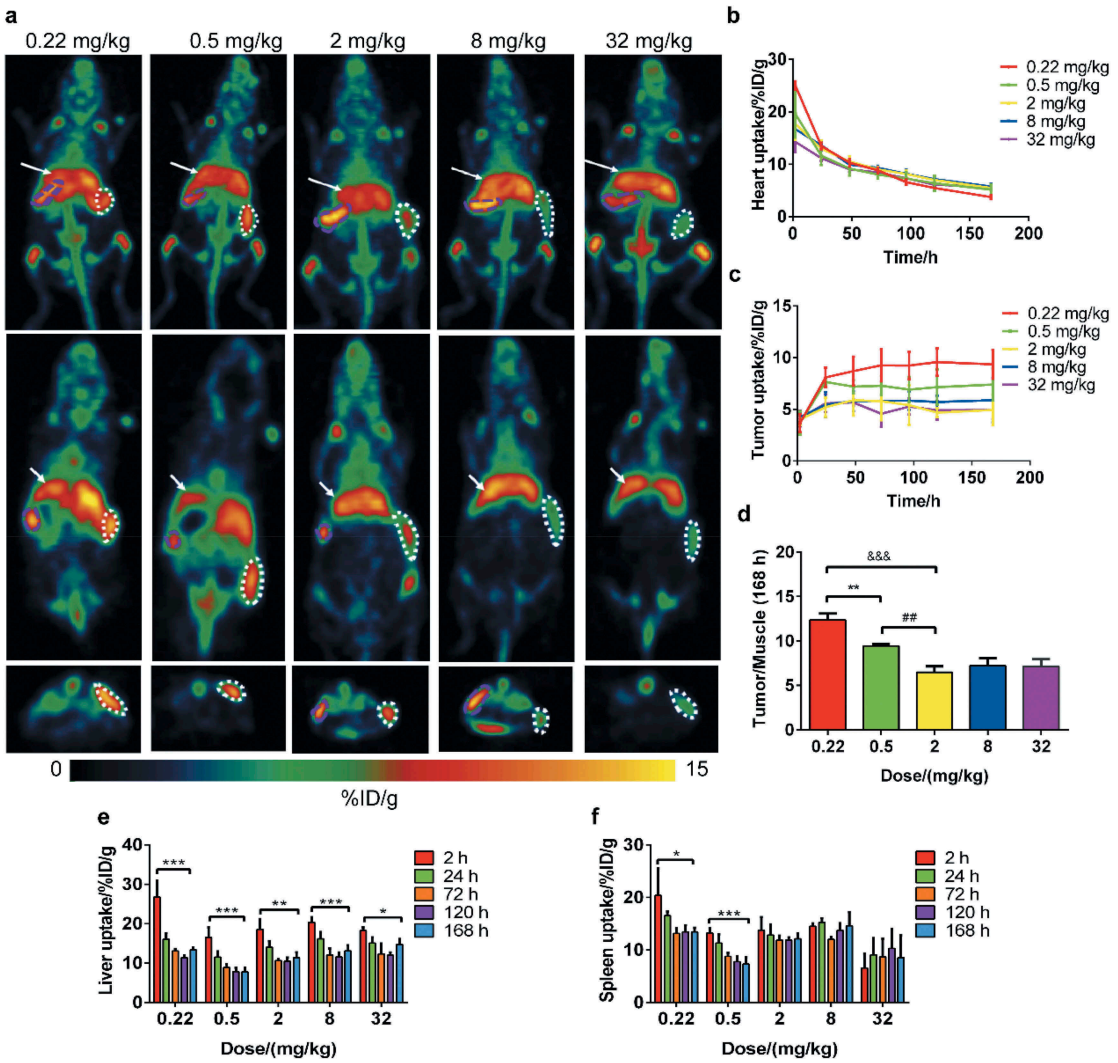

Figure 1. Results of dose escalation PET imaging with ^{89}Zr-labeled IBI322. Maximum intensity projections (MIPs) of a humanized transgenic mouse (B-hCD47; genotype: h/h) bearing an MC38 tumor (hCD47 and hPDL1) (above) and coronal (middle) and transverse (below) tomograms of the tumor at 168 h. The white arrow indicates the ROI of the liver, the white dotted line indicates the ROI of the tumor, and the purple dotted line indicates the ROI of the spleen (a). Images are parameterized as %ID/g. Time-activity curves of the heart (b) and tumor (c) for each group. (d) The tumor/muscle ratios of each group at 168 h. **: $p < .01$, group 1 vs group 2, ##: $p < .01$, group 2 vs group 3, &&&: $p < .001$, group 1 vs group 3. Histograms of liver (e) and spleen (f) uptake for each group. *: $p < .05$, 2 h vs 168 h, **: $p < .01$, 2 h vs 168 h, ***: $p < .001$, 2 h vs 168 h.

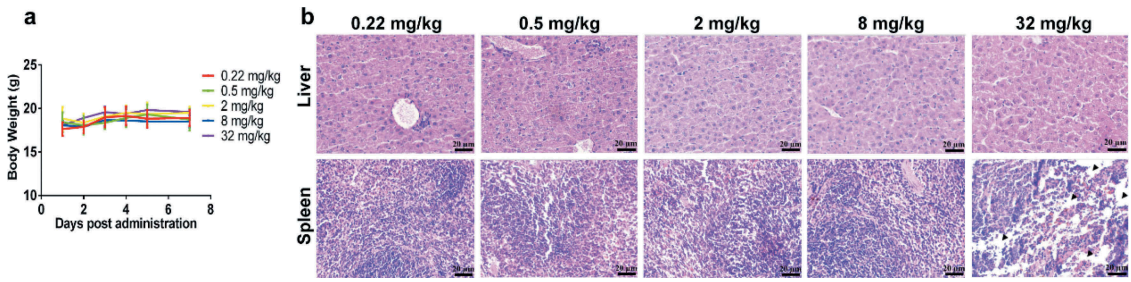

Figure 2. Results of the safety assessment from dose escalation PET imaging. The body weights of each group over the 7 d after administration (a). Histograms of liver (b) and spleen (c) uptake after intravenous injection of ^{89}Zr-labeled IBI322. H&E staining of liver and spleen sections from each group. (Scale bar: 200 μm) (d). The black arrow indicates partially necrotic regions of the spleen.

was higher than in the brain, muscle, stomach, lung, and other tissues. High and persistent radioactive concentrations were also observed in the liver (10.15 ± 1.14 at 168 h) and spleen (7.87 ± 0.07 at 168 h) (Figure 3(a)). The tumor uptake %ID/g was 9.31 ± 1.10, which further confirmed that IBI322 has excellent tumor-targeting properties. Additional

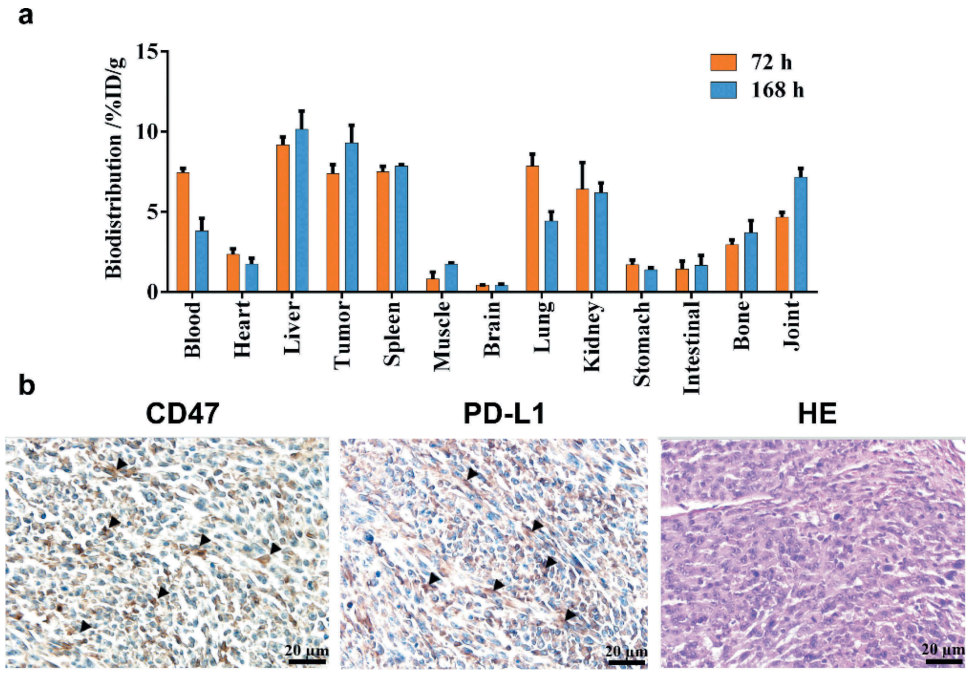

Figure 3. Biodistribution results. Tissue uptake (%ID/g) with the administration of 0.5 mg/kg ^{89}Zr-labeled IBI322 at 72 h and 168 h in transgenic mice (B-hCD47; genotype: h/h) bearing an MC38 tumor (hCD47 and hPDL1) (a). CD47 and PD-L1 IHC staining and H&E staining of the tumors (Scale bar: 200 μm) (b). Black arrow indicates positive expression.

ex vivo IHC showed abundant CD47 and PD-L1 expression in the tumors, with normal morphology (Figure 3(b)).

Pharmacokinetics and correlation analysis

Radio-HPLC analysis confirmed that ^{89}Zr-Df-IBI322 remained stable in the circulating blood for 168 h (Supplemental Figure 3c).

Figure 4(a) shows the curves of the serum concentration and blood/heart equivalent concentration with time. The PK parameters for administration with 0.5 mg/kg measured by an ELISA and the ex vivo blood equivalent concentrations are shown in Table 2.

The Pearson correlation coefficients between the serum concentration analyzed with ELISA and blood or heart uptake

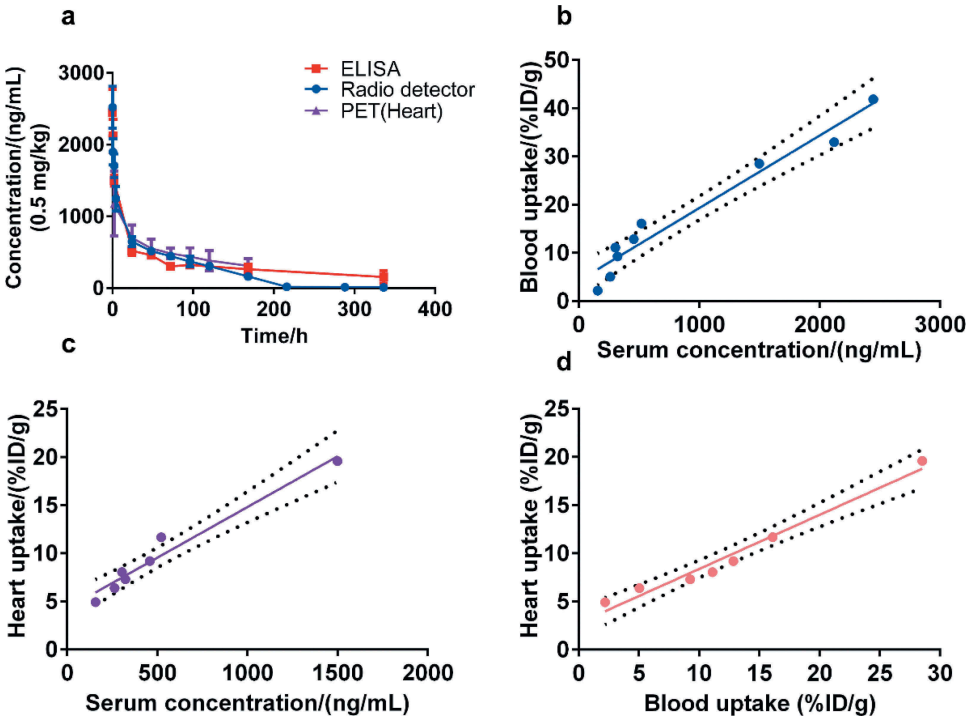

Figure 4. Results of the pharmacokinetics study. Curves show the serum concentration/blood and heart equivalent concentration over time analyzed by ELISA, radio detector, and PET imaging, respectively (a). (b to d) Pearson correlation analysis and linear regression fitting curves along the serum concentration (ng/mL) by ELISA, the blood uptake (%ID/g) determined by radio detector, and the heart uptake (%ID/g) determined by PET imaging. The dotted line represents the 95% confidence interval.

(%ID/g) were 0.977 and 0.980, respectively. High correlations existed among the serum concentration, blood, and heart uptake (%ID/g) (Figure 4b-d). Hence, the heart uptake from noninvasive PET imaging can replace the plasma concentration determined by ELISA for Patlak analysis, yielding a modified Patlak model.

Dose-dependent target engagement

The results of the dose-escalation study suggested that the target was saturated at doses greater than 2 mg/kg. To quantify the dose-dependency, a modified Patlak model was used to model irreversible tumor accumulation for each dose group (Figure 5(a)). For groups 1 through 5, the parameters fitted by the linear regression method are shown in Table 3. The fitting equation shows that the intercept (A') of each group was basically the same, while the slope (B') varied with the dose.

Furthermore, the fitted dose-inhibition curve between tumor engagement and the administration dose was compatible, with an ID50 of 0.38 mg/kg, an ID90 of 0.63 mg/kg and a nonspecific tumor accumulation of ~35% (Figure 5(b)).

Preliminary pharmacodynamics study

The tumor growth curve is shown in Figure 6, and the tumor growth inhibition (TGI, %) value for the IBI322 group was 112%. The optimal PD results were presented at the exploratory ID50 dose with an intra-abdominal injection once every 2 d for 7 times.

Discussion

PET imaging with a ^{89}Zr-labeled mAb may be used to gain better insight into the in vivo behavior of antibodies.[1,12,13] For any immunotherapeutic antibody evaluation, the first and foremost issue is to assess target saturation, which is helpful for effective therapy dose selection. In this study, dose escalation PET imaging was performed, and the dose-dependent target engagement was first evaluated for a BsAb.

The biodistribution and PET imaging studies showed that ^{89}Zr-Df-IBI322 specifically accumulated in tumors. Since the specific uptake was measured by comparing percentages of the injected dose per gram of tissue (%ID/g) in the tumor vs. other tissues in Figure 1, the volume of the tumor has little effect on specific uptake. Moreover, there was no significant difference in tumor volume among dosage groups during the imaging period (168 h). In addition to target tissues, similar to most mAbs, high and persistent uptake was observed in the liver.[17,23]

As CD47 is widely expressed in RBCs, radioactivity was also concentrated in the spleen. However, in contrast to the gradual decreasing trends of the heart, liver, and other tissues with abundant blood, the opposite trend was observed in the spleen in the highest dose group (32 mg/kg). Taking into consideration the spleen IHC results showing partial necrosis, and that the CD47 checkpoint is also overexpressed in T lymphocytes in transgenic animal models, we speculated that the abnormal gradually increasing trend of spleen uptake in the highest dosage group (32 mg/kg) may be related to safety; thus, the spleen may be an immune response tissue. Overall safety must, of course, be determined by the long-term monitoring, but PET imaging with ^{89}Zr-labeled antibody is expected to be a valuable noninvasive approach for whole-body safety prediction for IBI322.

A systematic correlation analysis was performed for the PK study of IBI322 using three methods: serum ELISA, ex vivo blood radioactive uptake (%ID/g) quantified with a gamma counter, and in vivo uptake (%ID/g) of the heart determined by PET imaging. For the same blood sample, the whole blood concentration (analyzed by a radioactive detector) was 14-47% higher than the serum concentration (quantified with ELISA) from 2 h to 96 h post injection (see Supplementary Table 1), and the AUC 0-t/AUC 0-inf_obs quantified by radioactivity detection was higher than the ELISA result (Table 2), which revealed that the anti-CD47 /PD-L1 BsAb might specifically bind to the RBCs.

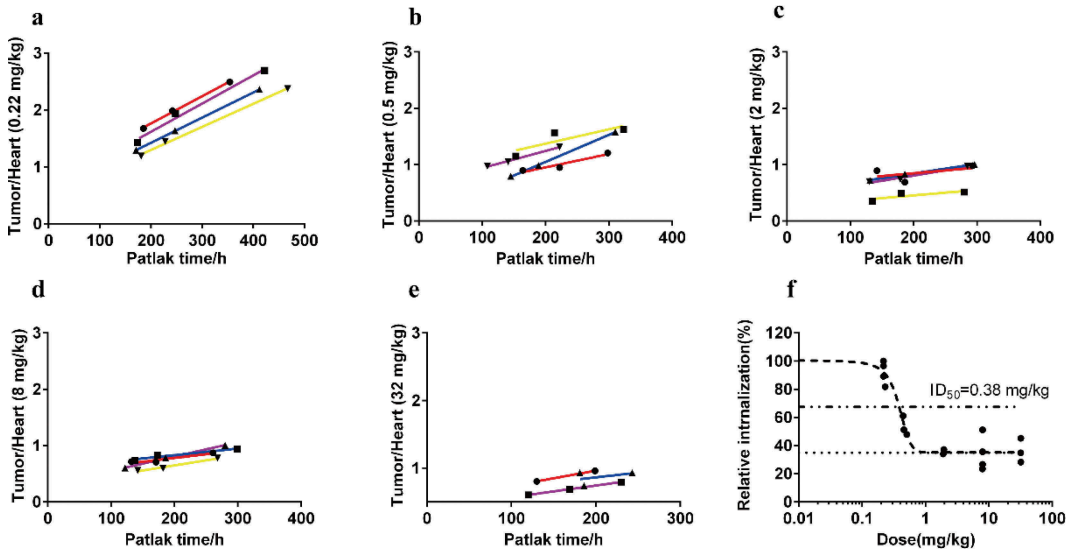

Figure 5. Modified Patlak plots for all dose groups (a-e) and dose-dependent tumor engagement curve (f).

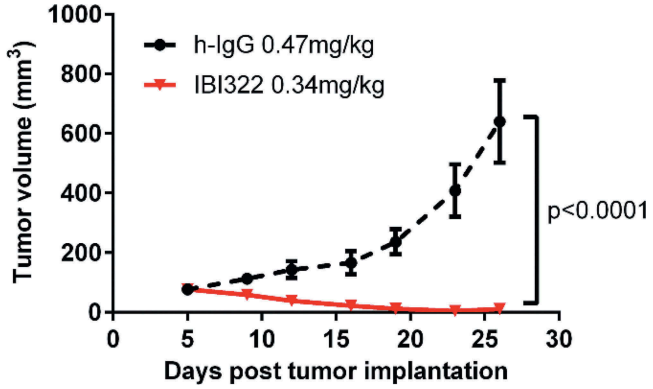

Figure 6. Preliminary pharmacodynamic results in NOD/SCID models bearing Raji/PD-L1 tumors (n = 6).

A key point of the modified Patlak model proposed is that a strong correlation was observed between the in vivo heart uptake from PET imaging and the ex vivo serum concentration analyzed by ELISA. Additionally, the AUC was fitted by the corresponding whole blood (for radio detector and PET imaging) or serum concentration (ELISA) using equation (1). According to equation (1) to (4) of the target engagement analysis, we inferred that under the condition that the radioactive component does not affect the blood concentration or can be calibrated, this noninvasive-modified Patlak model might be constrained to biologics with a similar convenient expression pattern.

Using our Patlak model, the dose-dependent target engagement of IBI322 can be assessed. The estimated ID90 for IBI322 is ~0.63 mg/kg, which is considerably lower than that of most mAbs (i.e., 18 mg/kg).[4] However, with dose escalation after target saturation, safety hazards may occur in normal tissues. Hence, the balance of efficacy and safety is more critical for BsAbs than for canonical mAbs.

For the narrow therapy windows and low effective doses of tumor-specific immunotherapeutic drugs, a high specific activity for a radiolabelled molecular probe is a prerequisite for PET imaging. In this study, we optimized the radiolabelling process to obtain a higher specific activity of ^{89}Zr-labeled IBI322 (4.4 μg per animal), which is far less than the conventional masses of mAbs (16.7 μg per animal).[24] The radiolabelling method is very important for the integration of diagnosis and treatment in future clinical trials of IBI322.

For better clinical translation, humanized transgenic animals were used for a dose escalation PET study.[25] As IBI322 targets both PD-L1 and CD47, the latter is distributed in tumor and human blood, but does not exist in the mouse circulatory system. Human CD47 was knocked into the mouse genome to generate this genetically modified animal model, thus allowing the mice to bind human antibodies with human drug metabolism capacities and toxicological phenotypes similar to those of humans. Therefore, the PK results, tumor and normal tissue distributions, and target engagement assessment of IBI322 have high clinical predictability.

There are, however, some limitations to this study. First, dual targets of IBI322 were considered as a whole in the current Patlak graphical model analysis; the validity of assumption needs to be verified. For both BsAbs and canonical mAbs, target saturation is an important parameter for effective therapy dose selection.[9,26] According to previous reports,[1,4,27] the low radiolabelled dose (0.22 mg/kg) was set as a baseline, and using dynamic dose escalation PET imaging, exploratory ID50, and ID90 values were obtained for IBI322 dose selection. Second, the PET PK study was observed until 168 h, but this window was not long enough to monitor the therapeutic response. Combined with the preliminary PD study (0.34 mg/kg, seven times), we confirmed that the dose prediction was rational. To establish PK/PD modeling for this BsAb, longitudinal PD as well as PK studies should be performed in the same humanized models. Third, the correlation between the radioactive detector and the ELISA method in the PK study was carried out only at a single dose (0.5 mg/kg). For systematic verification, further investigations will be evaluated at other dose levels in future studies.

In conclusion, this ^{89}Zr-labeled IBI322 PET PK imaging and preliminary PD study demonstrated the concept and feasibility of using noninvasive PET imaging to balance the safety and effectiveness of a treatment. Through systematic methodological verification, dose escalation PET imaging of a radiolabelled antibody is promising for PK/PD modeling and safety prediction of tumor immunotherapeutic drugs. This method will be important for selecting a rational dose in preclinical and clinical trials.

Materials and methods

Cell lines

All cell lines were purchased from American Type Culture Collection (ATCC). The MC38-PD-L1-CD47 co-expressed cell line and the Raji-PD-L1 overexpressed cell line were generated by lentivirus using a standard protocol. CD47 and PD-L1 expression levels in MC38 cells were confirmed by flow cytometry analysis before xenografts were performed (Supplemental Figure 1).

Animal models

Thirty-eight female transgenic mice (B-hCD47; genotype: h/h) aged 6–8 weeks were obtained from Beijing Biocytogen Co., Ltd. for dose escalation PET imaging, biodistribution, and PK studies. Twelve female NOD-SCID mice used for preliminary PD studies were purchased from Beijing Vital River Laboratory Animal Technology Co., Ltd. The mice were housed in individual ventilated cages at the Laboratory Animal Center of the Jiangsu Institute of Nuclear Medicine (Wuxi, China). To establish tumors, MC38-PD-L1-CD47 co-expressed cells ($2*10^6$ cells per animal) and PD-L1-expressing Raji cells ($9*10^6$ cells per animal) were injected subcutaneously into the right flanks of transgenic mice and NOD-SCID mice, respectively.

All procedures were approved by the Institutional Animal Care and Ethics Committee of Jiangsu Institute of Nuclear Medicine (Wuxi, China). Mice were anesthetized with continuously inhaled isoflurane (1.5-2%).

Conjugation and characterization

IBI322 was conjugated to *p*-SCN-deferoxamine (DFO) (Macrocyclics, USA) using traditional methods with some modifications.[28] Briefly, a nine-fold molar excess of DFO (in 20–30 µL dimethyl sulfoxide) was added to the antibody and stirred slowly at 37°C. After 90 min of reaction, a Df-IBI322 solution was purified using a PD-10 column (GE Healthcare).

The affinity of Df-IBI322 was determined with biolayer interferometry (Pall: OctetRED96). Df-IBI322 was immobilized on an AHC biosensor (Forte Bio, USA), bound to human CD47-His (ACRO Biosystems, USA) and human PD-L1 (ACRO Biosystems, USA) in solution, and finally dissociated in sample dilution buffer (1× Phosphate Buffered Saline with 0.1% bovine serum albumin and 0.05% Tween-20). All raw data were fitted using a 1:1 binding model with ForteBio data analysis software (version: 7.0).

^{89}Zr-radiolabelling

^{89}Zr-oxalate was obtained from Perkin Elmer, Inc. Df-IBI322 was radiolabeled with ^{89}Zr using a method previously reported with some modifications.[29] Briefly, 40–60 µL of ^{89}Zr-oxalate stock solution (~50–75 MBq) was diluted with a nine-fold volume of 0.2 M HEPES, the pH was adjusted to 7.0 with 0.1 M Na_2CO_3 solution, and Df-IBI322 was then added and incubated for 1 h at 37°C at ~50–65 GBq/µmol. Amicon Ultra-2 centrifugal filters (0.5 mL and 30 kDa MWCO; Millipore) were used to purify and concentrate ^{89}Zr antibodies with 0.15 M acetate buffer (pH 7.2) as the solvent, and the radiolabelling yield of ^{89}Zr-labeled IBI322 was measured by radio-instant thin-layer chromatography (radio-iTLC, Bioscan Inc.) using 50 mM citrate buffer at pH 5.0 as the mobile phase and glass fiber paper as the carrier.

The radiochemical purity was determined with HPLC on a Waters 1525 instrument with an online radioactivity detector (Radiomatic 610TR, Perkin Elmer) using an SEC chromatogram (G3000SWXL, TOSOH). The stability of ^{89}Zr-labeled IBI322 (~1.85 MBq) in 0.15 M acetate buffer (500 µL, pH 7.2) at 4°C for 168 h and in human serum (500 µL) at 37°C for 72 h was assessed using radio-iTLC (Bioscan Inc.) and a gamma counter (2480 WIZARD2, Perkin Elmer, Inc.).

Dose escalation PET imaging study

The dose-escalation study design is shown in Table 1 (four animals per group). All animals were imaged with microPET (Inveon, Siemens) at 2, 24, 48, 72, 96, 120, and 168 h after intravenous injection. The ordered subset expectation maximization 3D (OSEM3D) algorithm was used to reconstruct the PET data. The percentages of injected dose per gram of tissue (%ID/g) in ROIs were analyzed by an Inveon Research Workplace ASIPro (Siemens Medical Solutions) workstation.

Table 1. Dose escalation study design (n = 4).

Group	Activity (MBq)	Antibody mass of ^{89}Zr-Df-IBI322 per animal (µg)	Unlabeled IBI322 per animal (µg)	Dose (mg/kg)
1	1.41 ± 0.08	4-5	0	0.22
2	3.36 ± 0.08	8-10	0	0.5
3	3.02 ± 0.06	8-10	30	2
4	3.04 ± 0.10	8-10	150	8
5	3.04 ± 0.16	8-10	630	32

Table 2. Pharmacokinetics parameters.

Parameter	Unit	ELISA	Radio detector	PET (Heart)
t1/2	h	155.13	124.98	145.41
AUC 0-t	ng/ml*h	127291.32	223540.97	88232.42
AUC 0-inf_obs	ng/ml*h	137922.68	265996.38	153726.56
AUMC 0-inf_obs	ng/ml*h^2	2.658E+07	4.475E+07	3.057E+07
MRT 0-inf_obs	h	192.73	165.39	198.84

Table 3. Fitting parameters of each group with the modified Patlak model.

Group	Dose (mg/kg)	A′	B′
1	0.22	0.6881	0.004284
2	0.5	0.5552	0.002991
3	2	0.4388	0.001494
4	8	0.4229	0.001722
5	32	0.4804	0.001797

Safety

The body weight, animal survival condition, and H&E staining of the liver/spleen were determined in the preliminary safety assessment.

Biodistribution

To further confirm the biodistribution of IBI322, six animals were sacrificed at 72 and 168 h (n = 3). Approximately 0.5 mg/kg ^{89}Zr-Df-IBI322 (3.0–3.7 MBq per animal) was administered intravenously. Tumors and other organs were collected, weighed immediately, and assessed with a gamma counter (2480 WIZARD,[2] Perkin Elmer). The tissue uptake (%ID/g) was calculated.

Additionally, the tumor tissues were analyzed by IHC to detect the presence of CD47 and PD-L1 receptors using anti-CD47 (175388, Abcam) and anti-PD-L1 (205921, Abcam) primary antibodies. Routine H&E staining was also performed.

Pharmacokinetics

Three methods were used in the PK study: 1) the serum concentration was quantified with an ELISA, 2) ex vivo blood radioactive uptake (%ID/g) was quantified with a gamma counter, and 3) in vivo uptake (%ID/g) of the heart was determined by PET imaging.

For ex vivo serum ELISA analysis and radiolabelled blood uptake detection, 12 animals were used and intravenously injected with ^{89}Zr-Df-IBI322 (0.5 mg/kg, 3.0–3.7 MBq per animal). Blood samples were collected from the eyelids (300–-500 µL per animal) at 5 min, 30 min, 2 h, 24 h, 48 h, 72 h, 96 h, 168 h, 336 h, and 504 h after injection, and ~10–20 µL was used for ^{89}Zr-labeled IBI322 analysis with a gamma counter (2480 WIZARD2, Perkin Elmer). The remaining blood samples were then centrifuged immediately, and serum was used for unlabeled IBI322 analysis with an indirect antigen ELISA using a microplate reader (MULTISKAN FC, Thermo) to quantify the serum IBI322 concentrations (ng/mL). An indirect antigen ELISA was used to detect IBI322. The capture

agent was recombinant human PD-L1 (ACRO Biosystems; PD1-H5229), which was coated onto 96-well ELISA plates. Following overnight incubation, the plates were blocked, and the samples were added. Captured IBI322 was detected by an horseradish peroxidase-conjugated anti-human antibody (Sigma; A0293). Radioactive component analysis of serum was also performed with an HPLC instrument (Waters 1525) equipped with an online radioactivity detector (Radiomatic 610TR, Perkin Elmer) and gamma counter (2480 WIZARD2, Perkin Elmer).

For in vivo PK investigations with PET imaging, four animals were administered ^{89}Zr-Df-IBI322 (0.5 mg/kg, 3.0–3.7 MBq per animal). The heart was selected as the ROI for a noninvasive PK analysis, and the uptake (%ID/g) was then calculated.

Combined with the administration information (amount of protein and dose of radioactivity), the %ID/g results of ex vivo blood uptake and in vivo heart uptake could be converted into equivalent concentrations (ng eq./mL). A noncompartmental analysis was performed for plasma concentration determination by ELISA, and blood equivalent concentrations were determined with a radio detector using linear trapezoidal fitting with Phoenix WinNonLin (version: 6.4).

Pearson correlation analyses of the results of the above three methods were performed with SPSS 19 software.

Modified Patlak model for target engagement

For target saturation assessment with ^{89}Zr-immunoPET, previous studies have reported that Patlak modeling can be used to separate the specific and nonspecific components of the tumor uptake.[1,30] As a residualizing radionuclide, ^{89}Zr remains in cells after antibody internalization; thus, the specific part is related to the cumulative exposure of bound and/or degraded antibody over time, and the nonspecific part is associated with the plasma concentration and unbound antibody within the interstitial spaces of tissues. Because of the competition for receptor binding, the uptake of the target is decreased with co-injection of unlabeled antibodies. Thus, a low radiolabelled dose can be set as a baseline scan, and dose-dependent target engagement can be quantitatively evaluated by Patlak analysis by performing dynamic PET imaging.[31] With this model, the tumor uptake (%ID/g) can be defined as a function of the plasma radioactivity concentration Cp(t) using the following equation:[4]

$$\text{Tumor uptake}(\%\text{ID/g}) = \text{A} * \text{C}p(\text{t}) + \text{B}* \int_0^t Cp(\tau)d\tau \quad (1)$$

However, this classic Patlak model also requires continuous collection of blood for plasma analysis, which is difficult to obtain with small animals. In this study, a modified noninvasive Patlak model was proposed and verified. According to the results of this study and other previous reports,[17] the ^{89}Zr-labeled antibody remained stable in the circulating blood within 168 h from radio-HPLC analysis (Supplemental Figure 3c). Additionally, a high correlation was observed between the ex vivo plasma concentration quantified with an ELISA and the in vivo heart uptake (%ID/g) with PET imaging. Equation (1) can be modified as follows:

$$\text{Tumor uptake}(\%\text{ID/g}) = \text{A}' * \text{Heart uptake}(\%ID/g)(\text{t}) + \text{B}'* \int_0^t Heart\ uptake(\%ID/g)(\tau)d\tau \quad (2)$$

Equation (2) can be transformed into:

$$\text{Tumor uptake}(\%\text{IDg})/\text{Heart uptake}(\%ID/g)(\text{t}) = \text{A}' + \text{B}'*AUC(t)/\text{Heart uptake}(\%ID/g)(\text{t}) \quad (3)$$

where

A' = intercept, associated with nontarget binding components;

B' = slope, related to receptor-binding components followed by internalization after binding to receptors;

AUC(t) = area under heart uptake (%ID/g)-time curve (0-t).

As all tumor models were established using the same method, we assumed that each tumor exhibited the same level of CD47/PDL1 expression. The lowest radiolabelled dose (~0.22 mg/kg) was set as the baseline scan. The B'-value (slope) for each co-injection group in the dose-escalation study can be calculated as a percentage of baseline, and with the baseline dose internalization rate set to 100%, according to a previously described method,[4] the relative values were plotted against mass doses and fitted to a theoretical dose-inhibition curve. The constant fitting formula term indicates nonspecific internalization:

$$\text{R}(\%) = \text{Rnsp} + (100 - \text{Rnsp})/\left(1 + 10((\text{LogID50} - \hat{\text{D}}\text{ose})*\text{HillSlope})\right) \quad (4)$$

where

R = ratio of the co-injection B' value to the baseline B' value, called the 'relative internalization rate', and is expressed as a percentage;

Rnsp = expected percent ratio at total inhibition of CD47/PDL1 receptor internalization;

HillSlope = steepness of the curve.

From this curve, target-mediated 50% and 90% inhibitory mass doses (ID50 and ID90) of IBI322 and the nonspecific internalization of target-mediated uptake of ^{89}Zr-labeled IBI322 can be obtained.

Preliminary pharmacodynamics study

According to the predicted efficacy dose, the NOD-SCID mice bearing PD-L1-expressing Raji tumors were randomly divided into two groups (n = 6) on the fifth-day post tumor implantation: the control group with 0.47 mg/kg h-IgG (Equitech-Bio) and the IBI322 group with 0.34 mg/kg. Intra-abdominal injection was performed once every 2 d for 7 times, and the tumor volumes were monitored twice a week for 21 d. At the end of the experiment, the tumor growth inhibition value (TGI, %) in each group was calculated.

Statistical analysis

Quantitative data are expressed as the mean±standard deviation (SD), with all error bars denoting the SD. The means were compared using Student's t test, and p values less than 0.05 were considered statistically significant.

Abbreviations

^{89}Zr	^{89}Zirconium
%ID/g	Percentages of injected dose per gram of tissue
ADCs	Antibody-drug conjugates
ATCC	American Type Culture Collection
BED	Biologically effective dose
BsAbs	Bispecific antibodies
DFO	*p*-SCN-deferoxamine
ELISA	Enzyme-linked immunosorbent assay
FIH	First-in-human
H&E	Haematoxylin/eosin
HPLC	High-performance liquid chromatography
IHC	immunohistochemistry
mAbs	Monoclonal antibodies
OSEM3D	Ordered subset expectation maximization 3D
PD	Pharmacodynamic
PET	Positron emission tomography
PK	Pharmacokinetic
Radio-iTLC	Radio-instant thin-layer chromatography
RBCs	Red blood cells
ROIs	Regions of interest
SEC	Size exclusion chromatography
TGI	Tumor growth inhibition value

Acknowledgments

We thank AJE for English language editing of our manuscript.

Author contributions

YW, DHP, and CRH designed and performed all experiments, and wrote the manuscript. BLC, SXZ, MW, and JJL assisted in the cell culture, establishment of animal model, characterization of BsAb and DFO conjugation BsAb and enzyme-linked immunosorbent assay. MZL, LZW, and YCB labeled Df-IBI322 with ^{89}Zr and performed part of the in vivo experiments. XYW and JJY helped to revise the manuscript. LYM and MY designed and supervised the project. All authors have reviewed and approved the manuscript.

Disclosure of potential conflicts of interest

No potential conflicts of interest were disclosed.

Funding

This work was financially supported by the National Significant New Drugs Creation Program (2017ZX09304021), the National Natural Science Foundation of China (31971316, 51803082, 81773820), the Jiangsu Provincial Medical Innovation Team (CXTDA2017024), the Leading technology foundation research project of Jiangsu province (BK20192005), and the Special Research Fund of Wu Jieping Medical Foundation of Chinese Society of Clinical Pharmacy (320.6750.19090-50).

References

1. Reilly RM. ImmunoPET to optimize the dose of monoclonal antibodies for cancer therapy - How much is enough? J Nucl Med. 2019;60:899–901. doi:10.2967/jnumed.119.225854.
2. Saber H, Del Valle P, Ricks TK, Leighton JK. An FDA oncology analysis of CD3 bispecific constructs and first-in-human dose selection. Regul Toxicol Pharmacol. 2017;90:144–52. doi:10.1016/j.yrtph.2017.09.001.
3. Saber H, Gudi R, Manning M, Wearne E, Leighton JK. An FDA oncology analysis of immune activating products and first-in-human dose selection. Regul Toxicol Pharmacol. 2016;81:448–56. doi:10.1016/j.yrtph.2016.10.002.
4. Menke-van der Houven van Oordt CW, McGeoch A, Bergstrom M, McSherry I, Smith DA, Cleveland M, Al-Azzam W, Chen L, Verheul H, Hoekstra OS, et al. ImmunoPET imaging to assess target engagement: experience from (89)Zr-anti-HER3 mAb (GSK2849330) in patients with solid tumors. J Nucl Med. 2019;60:902–09. doi:10.2967/jnumed.118.214726.
5. Stewart JJ, Green CL, Jones N, Liang M, Xu Y, Wilkins DE, Moulard M, Czechowska K, Lanham D, McCloskey TW, et al. Role of receptor occupancy assays by flow cytometry in drug development. Cytometry B Clin Cytom. 2016;90(2):110–16. doi:10.1002/ccc.21355.
6. Vainshtein I, Schneider AK, Sun B, Schwickart M, Roskos LK, Liang M. Multiplexing of receptor occupancy measurements for pharmacodynamic biomarker assessment of biopharmaceuticals. Cytometry B Clin Cytom. 2016;90(2):128–40. doi:10.1002/cyto.b.21319.
7. Litwin V, Green C, Stewart JJ. Receptor occupancy by flow cytometry. Cytometry B Clin Cytom. 2016;90(2):108–09. doi:10.1002/cyto.b.21364.
8. Liang M, Schwickart M, Schneider AK, Vainshtein I, Del Nagro C, Standifer N, Roskos LK. Receptor occupancy assessment by flow cytometry as a pharmacodynamic biomarker in biopharmaceutical development. Cytometry B Clin Cytom. 2016;90(2):117–27. doi:10.1002/cyto.b.21259.
9. Deng R, Bumbaca D, Pastuskovas CV, Boswell CA, West D, Cowan KJ, Chiu H, McBride J, Johnson C, Xin Y, et al. Preclinical pharmacokinetics, pharmacodynamics, tissue distribution, and tumor penetration of anti-PD-L1 monoclonal antibody, an immune checkpoint inhibitor. MAbs. 2016;8(3):593–603. doi:10.1080/19420862.2015.1136043.
10. Meno-Tetang GM, Lowe PJ. On the prediction of the human response: a recycled mechanistic pharmacokinetic/pharmacodynamic approach. Basic Clin Pharmacol Toxicol. 2005;96(3):182–92. doi:10.1111/j.1742-7843.2005.pto960307.x.
11. Schlucker S, Salehi M, Bergner G, Schutz M, Strobel P, Marx A, Petersen I, Dietzek B, Popp J. Immuno-surface-enhanced coherent anti-stokes Raman scattering microscopy: immunohistochemistry with target-specific metallic nanoprobes and nonlinear Raman microscopy. Anal Chem. 2011;83(18):7081–85. doi:10.1021/ac201284d.
12. Alsaid H, Skedzielewski T, Rambo MV, Hunsinger K, Hoang B, Fieles W, Long ER, Tunstead J, Vugts DJ, Cleveland M, et al. Non invasive imaging assessment of the biodistribution of GSK2849330, an ADCC and CDC optimized anti HER3 mAb, and its role in tumor macrophage recruitment in human tumor-bearing mice. PLoS One. 2017;12(4):e0176075. doi:10.1371/journal.pone.0176075.
13. Burvenich IJG, Lee FT, Cartwright GA, O'Keefe GJ, Makris D, Cao D, Gong S, Chueh AC, Mariadason JM, Brechbiel MW, et al. Molecular imaging of death receptor 5 occupancy and saturation kinetics in vivo by humanized monoclonal antibody CS-1008. Clin Cancer Res. 2013;19(21):5984–93. doi:10.1158/1078-0432.Ccr-12-3104.
14. Orcutt KD, Adams GP, Wu AM, Silva MD, Harwell C, Hoppin J, Matsumura M, Kotsuma M, Greenberg J, AM S, et al. Molecular simulation of receptor occupancy and tumor penetration of an

antibody and smaller scaffolds: application to molecular imaging. Mol Imaging Biol. 2017;19(5):656–64. doi:10.1007/s11307-016-1041-y.
15. Heskamp S, Raave R, Boerman O, Rijpkema M, Goncalves V, Denat F. (89)Zr-Immuno-Positron Emission tomography in oncology: state-of-the-art (89)Zr radiochemistry. Bioconjug Chem. 2017;28(9):2211–23. doi:10.1021/acs.bioconjchem.7b00325.
16. Sugyo A, Aung W, Tsuji A, Sudo H, Takashima H, Yasunaga M, Matsumura Y, Saga T, Higashi T. Anti-tissue factor antibody-mediated immuno-SPECT imaging of tissue factor expression in mouse models of pancreatic cancer. Oncol Rep. 2019;41(4):2371–78. doi:10.3892/or.2019.7017.
17. Bensch F, van der Veen EL, Lub-de Hooge MN, Jorritsma-Smit A, Boellaard R, Kok IC, Oosting SF, Schröder CP, Hiltermann TJN, van der Wekken AJ, et al. (89)Zr-atezolizumab imaging as a non-invasive approach to assess clinical response to PD-L1 blockade in cancer. Nat Med. 2018;24(12):1852–58. doi:10.1038/s41591-018-0255-8.
18. England CG, Ehlerding EB, Hernandez R, Rekoske BT, Graves SA, Sun H, Liu G, McNeel DG, Barnhart TE, Cai W. Preclinical pharmacokinetics and biodistribution studies of 89Zr-Labeled pembrolizumab. J Nucl Med. 2017;58(1):162–68. doi:10.2967/jnumed.116.177857.
19. Mandikian D, Takahashi N, Lo AA, Li J, Eastham-Anderson J, Slaga D, Ho J, Hristopoulos M, Clark R, Totpal K, et al. relative target affinities of T-Cell-dependent bispecific antibodies determine biodistribution in a solid tumor mouse model. Mol Cancer Ther. 2018;17(4):776–85. doi:10.1158/1535-7163.MCT-17-0657.
20. Moek KL, Waaijer SJH, Kok IC, Suurs FV, Brouwers AH, Menke-van der Houven van Oordt CW, Wind TT, Gietema JA, Schröder CP, Mahesh SVK, et al. (89)Zr-labeled bispecific T-cell engager AMG 211 PET shows AMG 211 accumulation in CD3-rich tissues and clear, heterogeneous tumor uptake. Clin Cancer Res. 2019;25(12):3517–27. doi:10.1158/1078-0432.CCR-18-2918.
21. Carrasquillo JA, Fine BM, Pandit-Taskar N, Larson SM, Fleming SE, Fox JJ, Cheal SM, O'Donoghue JA, Ruan S, Ragupathi G, et al. Imaging patients with metastatic castration-resistant prostate cancer using 89Zr-DFO-MSTP2109A anti-steap1 antibody. J Nucl Med. 2019;60(11):1517–23. doi:10.2967/jnumed.118.222844.
22. Yu S, Zhang J, Yan Y, Yao X, Fang L, Xiong H, Liu Y, Chu Q, Zhou P, Wu K. A novel asymmetrical anti-HER2/CD3 bispecific antibody exhibits potent cytotoxicity for HER2-positive tumor cells. J Exp Clin Cancer Res. 2019;38(1):355. doi:10.1186/s13046-019-1354-1.
23. Vugts DJ, Heuveling DA, Stigter-van Walsum M, Weigand S, Bergstrom M, van Dongen GA, Nayak TK. Preclinical evaluation of 89Zr-labeled anti-CD44 monoclonal antibody RG7356 in mice and cynomolgus monkeys: prelude to Phase 1 clinical studies. MAbs. 2014;6(2):567–75. doi:10.4161/mabs.27415.
24. Marquez BV, Ikotun OF, Zheleznyak A, Wright B, Hari-Raj A, Pierce RA, Lapi SE. Evaluation of (89)Zr-pertuzumab in Breast cancer xenografts. Mol Pharm. 2014;11(11):3988–95. doi:10.1021/mp500323d.
25. Shultz LD, Ishikawa F, Greiner DL. Humanized mice in translational biomedical research. Nat Rev Immunol. 2007;7(2):118–30. doi:10.1038/nri2017.
26. de Vries Schultink AHM, Doornbos RP, Bakker ABH, Bol K, Throsby M, Geuijen C, Maussang D, Schellens JHM, Beijnen JH, Huitema ADR. Translational PK-PD modeling analysis of MCLA-128, a HER2/HER3 bispecific monoclonal antibody, to predict clinical efficacious exposure and dose. Invest New Drugs. 2018;36(6):1006–15. doi:10.1007/s10637-018-0593-x.
27. Patlak CS, Blasberg RG, Fenstermacher JD. Graphical evaluation of blood-to-brain transfer constants from multiple-time uptake data. J Cereb Blood Flow Metab. 1983;3(1):1–7. doi:10.1038/jcbfm.1983.1.
28. Zeglis BM, Lewis JS. The bioconjugation and radiosynthesis of 89Zr-DFO-labeled antibodies. J Vis Exp. 2015:96. doi:10.3791/52521.
29. Deshayes E, Ladjohounlou R, Le Fur P, Pichard A, Lozza C, Boudousq V, Sevestre S, Jarlier M, Kashani R, Koch J, et al. Radiolabeled antibodies against mullerian-inhibiting substance receptor, Type II: new tools for a theranostic approach in ovarian cancer. J Nucl Med. 2018;59(8):1234–42. doi:10.2967/jnumed.118.208611.
30. Bergstrom M. The use of microdosing in the development of small organic and protein therapeutics. J Nucl Med. 2017;58(8):1188–95. doi:10.2967/jnumed.116.188037.
31. Ilan E, Velikyan I, Sandstrom M, Sundin A, Lubberink M. Tumor-to-blood ratio for assessment of somatostatin receptor density in neuroendocrine tumors using (68)Ga-DOTATOC and (68)Ga-DOTATATE. J Nucl Med. 2020;61(2):217–21. doi:10.2967/jnumed.119.228072.